Terrestrial matter effects on reactor antineutrino oscillations at JUNO or RENO-50: how small is small? *

Yu-feng Li(李玉峰)[1)] Yi-fang Wang(王贻芳)[2)] Zhi-zhong Xing(邢志忠)[3)]

[1] Institute of High Energy Physics, Chinese Academy of Sciences, Beijing 100049, China
[2] School of Physical Sciences, University of Chinese Academy of Sciences, Beijing 100049, China

Abstract: We have carefully examined, in both analytical and numerical ways, how small the terrestrial matter effects can be in a given medium-baseline reactor antineutrino oscillation experiment like JUNO or RENO-50. Taking the forthcoming JUNO experiment as an example, we show that the inclusion of terrestrial matter effects may reduce the sensitivity of the neutrino mass ordering measurement by $\Delta\chi^2_{\rm MO} \simeq 0.6$, and a neglect of such effects may shift the best-fit values of the flavor mixing angle θ_{12} and the neutrino mass-squared difference Δ_{21} by about 1σ to 2σ in the future data analysis. In addition, a preliminary estimate indicates that a 2σ sensitivity of establishing the terrestrial matter effects can be achieved for about 10 years of data taking at JUNO with the help of a suitable near detector implementation.

Keywords: terrestrial matter effects, reactor antineutrino oscillations

PACS: 14.60.Pq, 13.10.+q, 25.30.Pt **DOI:** 10.1088/1674-1137/40/9/091001

1 Introduction

The approved JUNO project in China is a flagship of the new-generation medium-baseline reactor antineutrino oscillation experiments [1, 2], and its primary physics target is to probe the intriguing neutrino mass ordering [3, 4] (i.e., whether $m_1 < m_2 < m_3$ or $m_3 < m_1 < m_2$). A similar project in South Korea, the RENO-50 experiment [5], has been proposed for the same purpose. Since the typical energies of electron antineutrinos produced from a reactor are around 4 MeV, terrestrial matter effects are expected to be negligibly small in any given $\overline{\nu}_{\rm e} \to \overline{\nu}_{\rm e}$ oscillation experiment. However, a careful examination of the sensitivity of measuring the neutrino mass ordering to the matter-induced contamination has been lacking, although some preliminary estimates of the matter effects on the leptonic flavor mixing angles and neutrino mass-squared differences have been made in this connection [6–8].

In the present work we aim to evaluate how small the terrestrial matter effects are and whether they can affect the precision measurements to be done in the JUNO and RENO-50 experiments. Our main results will be presented both numerically and in some useful and instructive analytical approximations. A remarkable observation is that the terrestrial matter contamination may give rise to a correction close to 1% to the quantity associated with a crucial judgement of whether the neutrino mass ordering is normal or inverted. Taking the JUNO experiment as an example, we show that the inclusion of terrestrial matter effects may reduce the sensitivity of the neutrino mass ordering measurement by $\Delta\chi^2_{\rm MO} \simeq 0.6$, and a neglect of such effects may shift the best-fit values of the flavor mixing angle θ_{12} and the neutrino mass-squared difference Δ_{21} by about 1σ to 2σ in future data analysis. Moreover, a preliminary estimate indicates that a 2σ sensitivity of establishing the terrestrial matter effects can be achieved for about 10 years of data taking at JUNO with the help of a suitable near detector implementation.

2 Analytical approximations

Let us begin with the effective Hamiltonian that is responsible for the propagation of *antineutrinos* in matter [9, 10]

Received 5 May 2016

∗ Supported by National Natural Science Foundation of China (11135009, 11305193), the Strategic Priority Research Program of the Chinese Academy of Sciences (XDA10010100) and the CAS Center for Excellence in Particle Physics

1) E-mail: liyufeng@ihep.ac.cn
2) E-mail: yfwang@ihep.ac.cn
3) E-mail: xingzz@ihep.ac.cn

$$\widetilde{\mathcal{H}}_{\rm eff} = \frac{1}{2E}\left[\widetilde{U}\begin{pmatrix}\widetilde{m}_1^2 & 0 & 0\\ 0 & \widetilde{m}_2^2 & 0\\ 0 & 0 & \widetilde{m}_3^2\end{pmatrix}\widetilde{U}^\dagger\right]$$

$$= \frac{1}{2E}\left[U\begin{pmatrix}m_1^2 & 0 & 0\\ 0 & m_2^2 & 0\\ 0 & 0 & m_3^2\end{pmatrix}U^\dagger - \begin{pmatrix}A & 0 & 0\\ 0 & 0 & 0\\ 0 & 0 & 0\end{pmatrix}\right], \quad (1)$$

where $\widetilde{U}$ (or U) and $\widetilde{m}_i$ (or m_i) stand respectively for the effective (or fundamental) lepton flavor mixing matrix and neutrino masses in matter (or in vacuum), and $A = 2\sqrt{2}\,G_{\rm F}N_{\rm e}E$ with $G_{\rm F}$ being the Fermi constant and $N_{\rm e}$ being the background density of electrons. In fact, A itself and the minus sign in front of A denote the charged-current contribution to the coherent $\overline{\nu}_{\rm e}{\rm e}^-$ forward scattering in matter. Given a constant matter profile which is a good approximation for the reactor-based antineutrino oscillation experiments, one may establish the exact analytical relations between $|U_{ei}|^2$ and $|\widetilde{U}_{ei}|^2$ as follows [11]:

$$\begin{aligned}
|\widetilde{U}_{\rm e1}|^2 &= +\frac{\Delta'_{21}\Delta'_{31}}{\widetilde{\Delta}_{21}\widetilde{\Delta}_{31}}|U_{\rm e1}|^2 + \frac{\Delta'_{11}\Delta'_{31}}{\widetilde{\Delta}_{21}\widetilde{\Delta}_{31}}|U_{\rm e2}|^2 + \frac{\Delta'_{11}\Delta'_{21}}{\widetilde{\Delta}_{21}\widetilde{\Delta}_{31}}|U_{\rm e3}|^2\,,\\
|\widetilde{U}_{\rm e2}|^2 &= -\frac{\Delta'_{22}\Delta'_{32}}{\widetilde{\Delta}_{21}\widetilde{\Delta}_{32}}|U_{\rm e1}|^2 - \frac{\Delta'_{12}\Delta'_{32}}{\widetilde{\Delta}_{21}\widetilde{\Delta}_{32}}|U_{\rm e2}|^2 - \frac{\Delta'_{12}\Delta'_{22}}{\widetilde{\Delta}_{21}\widetilde{\Delta}_{32}}|U_{\rm e3}|^2\,,\\
|\widetilde{U}_{\rm e3}|^2 &= +\frac{\Delta'_{23}\Delta'_{33}}{\widetilde{\Delta}_{31}\widetilde{\Delta}_{32}}|U_{\rm e1}|^2 + \frac{\Delta'_{13}\Delta'_{33}}{\widetilde{\Delta}_{31}\widetilde{\Delta}_{32}}|U_{\rm e2}|^2 + \frac{\Delta'_{13}\Delta'_{23}}{\widetilde{\Delta}_{31}\widetilde{\Delta}_{32}}|U_{\rm e3}|^2\,,
\end{aligned} \quad (2)$$

where $\widetilde{\Delta}_{ij} \equiv \widetilde{m}_i^2 - \widetilde{m}_j^2$ and $\Delta'_{ij} \equiv m_i^2 - \widetilde{m}_j^2$ as compared with the fundamental neutrino mass-squared differences $\Delta_{ij} \equiv m_i^2 - m_j^2$ (for $i,j = 1,2,3$). To see the matter effects hidden in $\widetilde{\Delta}_{ij}$ and Δ'_{ij} in a transparent way, we take into account their approximate expressions expanded in terms of two small parameters $\alpha \equiv \Delta_{21}/\Delta_{31}$ and $\beta \equiv A/\Delta_{31}$ in the normal neutrino mass ordering (i.e., $\Delta_{31} > 0$) case [12]:

$$\begin{aligned}
\widetilde{\Delta}_{21} &\simeq \Delta_{31}\left(1 - \frac{3}{2}|U_{\rm e3}|^2\beta\right)\epsilon\,,\\
\widetilde{\Delta}_{31} &\simeq \Delta_{31}\left[1 - \frac{1}{2}\alpha + \frac{1}{2}(1 - 3|U_{\rm e3}|^2)\beta\right.\\
&\quad \left. + \frac{1}{2}\epsilon + \frac{3}{4}|U_{\rm e3}|^2\beta(2\beta - \epsilon)\right],\\
\widetilde{\Delta}_{32} &\simeq \Delta_{31}\left[1 - \frac{1}{2}\alpha + \frac{1}{2}(1 - 3|U_{\rm e3}|^2)\beta - \frac{1}{2}\epsilon\right.\\
&\quad \left. + \frac{3}{4}|U_{\rm e3}|^2\beta(2\beta + \epsilon)\right];
\end{aligned} \quad (3)$$

and

$$\begin{aligned}
\Delta'_{11} &\simeq -\Delta_{31}\left[\frac{1}{2}\alpha - \frac{1}{2}(1 - |U_{\rm e3}|^2)\beta\right.\\
&\quad \left. - \frac{1}{2}\epsilon - \frac{1}{4}|U_{\rm e3}|^2\beta(2\beta - 3\epsilon)\right],\\
\Delta'_{12} &\simeq -\Delta_{31}\left[\frac{1}{2}\alpha - \frac{1}{2}(1 - |U_{\rm e3}|^2)\beta\right.\\
&\quad \left. + \frac{1}{2}\epsilon - \frac{1}{4}|U_{\rm e3}|^2\beta(2\beta + 3\epsilon)\right],\\
\Delta'_{13} &\simeq -\Delta_{31}(1 - |U_{\rm e3}|^2\beta + |U_{\rm e3}|^2\beta^2)\,,\\
\Delta'_{21} &\simeq +\Delta_{31}\left[\frac{1}{2}\alpha + \frac{1}{2}(1 - |U_{\rm e3}|^2)\beta\right.\\
&\quad \left. + \frac{1}{2}\epsilon + \frac{1}{4}|U_{\rm e3}|^2\beta(2\beta - 3\epsilon)\right],\\
\Delta'_{22} &\simeq +\Delta_{31}\left[\frac{1}{2}\alpha + \frac{1}{2}(1 - |U_{\rm e3}|^2)\beta\right.\\
&\quad \left. - \frac{1}{2}\epsilon + \frac{1}{4}|U_{\rm e3}|^2\beta(2\beta + 3\epsilon)\right],\\
\Delta'_{23} &\simeq -\Delta_{31}(1 - \alpha - |U_{\rm e3}|^2\beta + |U_{\rm e3}|^2\beta^2)\,,\\
\Delta'_{31} &\simeq +\Delta_{31}\left[1 - \frac{1}{2}\alpha + \frac{1}{2}(1 - |U_{\rm e3}|^2)\beta\right.\\
&\quad \left. + \frac{1}{2}\epsilon + \frac{1}{4}|U_{\rm e3}|^2\beta(2\beta - 3\epsilon)\right],\\
\Delta'_{32} &\simeq +\Delta_{31}\left[1 - \frac{1}{2}\alpha + \frac{1}{2}(1 - |U_{\rm e3}|^2)\beta\right.\\
&\quad \left. - \frac{1}{2}\epsilon + \frac{1}{4}|U_{\rm e3}|^2\beta(2\beta + 3\epsilon)\right],\\
\Delta'_{33} &\simeq +\Delta_{31}(|U_{\rm e3}|^2\beta + |U_{\rm e3}|^2\beta^2)\,,
\end{aligned} \quad (4)$$

where

$$\epsilon \equiv \sqrt{\alpha^2 + 2(|U_{\rm e1}|^2 - |U_{\rm e2}|^2)\alpha\beta + (1 - 2|U_{\rm e3}|^2)\beta^2}\,. \quad (5)$$

Note that the smallness of $|U_{\rm e3}|$ is already implied in making the above approximations. With the help of Eqs. (3) and (4), the expressions in Eq. (2) can be simplified to

$$\begin{aligned}
|\widetilde{U}_{\rm e1}|^2 &\simeq +\frac{\alpha + \beta + \epsilon}{2\epsilon}|U_{\rm e1}|^2 - \frac{\alpha - \beta - \epsilon}{2\epsilon}|U_{\rm e2}|^2\,,\\
|\widetilde{U}_{\rm e2}|^2 &\simeq -\frac{\alpha + \beta - \epsilon}{2\epsilon}|U_{\rm e1}|^2 + \frac{\alpha - \beta + \epsilon}{2\epsilon}|U_{\rm e2}|^2\,,\\
|\widetilde{U}_{\rm e3}|^2 &\simeq |U_{\rm e3}|^2
\end{aligned} \quad (6)$$

in the leading-order approximation [1)]. Given $A \sim 1.52 \times 10^{-4}$ eV^2 $Y_e\,(\rho/{\rm g/cm^3})\,(E/{\rm GeV}) \simeq 1.98 \times$

[1)] In the next-to-leading-order approximation one may obtain the analytical result $|\widetilde{U}_{\rm e3}|^2 \simeq (1 - 2\beta)|U_{\rm e3}|^2$. Since β is of $\mathcal{O}(10^{-4})$ as estimated in Eq. (7), $|\widetilde{U}_{\rm e3}|^2 \simeq |U_{\rm e3}|^2$ is actually an excellent approximation.

10^{-4} eV^2(E/GeV) for a realistic oscillation experiment [13], where $Y_e \simeq 0.5$ is the electron fraction and $\rho \simeq 2.6$ g/cm^3 is the typical matter density for an antineutrino trajectory through the Earth's crust [2], we find that β is much smaller than α in magnitude:

$$\alpha \simeq 3.12\times10^{-2}\times\frac{\Delta_{21}}{7.5\times10^{-5}\ \text{eV}^2}\times\frac{\pm2.4\times10^{-3}\ \text{eV}^2}{\Delta_{31}}\,,$$
$$\beta \simeq 3.29\times10^{-4}\times\frac{E}{4\ \text{MeV}}\times\frac{\pm2.4\times10^{-3}\ \text{eV}^2}{\Delta_{31}}\,. \quad (7)$$

In this case one may simplify the expression of ϵ in Eq. (5) as $\epsilon \simeq \alpha + (|U_{\rm e1}|^2 - |U_{\rm e2}|^2)\beta$ plus much smaller terms. Note that Eqs. (3), (4) and (6) are valid for a normal neutrino mass ordering. If an inverted neutrino mass ordering (i.e., $\Delta_{31} < 0$) is taken into account, the corresponding expressions can simply be obtained from the above equations with a straightforward replacement $\epsilon \to -\epsilon$.

In the standard parametrization of U [14], $|U_{\rm e1}| = \cos\theta_{12}\cos\theta_{13}$, $|U_{\rm e2}| = \sin\theta_{12}\cos\theta_{13}$ and $|U_{\rm e3}| = \sin\theta_{13}$. A global analysis of current neutrino oscillation data yields the best-fit values $\theta_{12} \simeq 33.5^\circ$ and $\theta_{13} \simeq 8.5^\circ$ [15–18], which are insensitive to the neutrino mass ordering. Therefore, $\epsilon \simeq \alpha + \beta\cos2\theta_{12}$ holds as a good approximation. Taking the same parametrization for the effective neutrino mixing matrix $\widetilde{U}$ in matter, one may link the effective flavor mixing angles $\widetilde{\theta}_{12}$ and $\widetilde{\theta}_{13}$ with the fundamental flavor mixing angles θ_{12} and θ_{13} via Eq. (6). Namely,

$$|\widetilde{U}_{\rm e1}|^2 \simeq \frac{\alpha+\beta\cos^2\theta_{12}}{\alpha+\beta\cos2\theta_{12}}|U_{\rm e1}|^2 + \frac{\beta\cos^2\theta_{12}}{\alpha+\beta\cos2\theta_{12}}|U_{\rm e2}|^2\,,$$
$$|\widetilde{U}_{\rm e2}|^2 \simeq \frac{\alpha-\beta\sin^2\theta_{12}}{\alpha+\beta\cos2\theta_{12}}|U_{\rm e2}|^2 - \frac{\beta\sin^2\theta_{12}}{\alpha+\beta\cos2\theta_{12}}|U_{\rm e1}|^2\,,$$
$$|\widetilde{U}_{\rm e3}|^2 \simeq |U_{\rm e3}|^2\,; \quad (8)$$

and thus we arrive at the $\widetilde{\theta}_{13} \simeq \theta_{13}$ and

$$\cos^2\widetilde{\theta}_{12} \simeq \frac{(\alpha+\beta)\cos^2\theta_{12}}{\alpha+\beta\cos2\theta_{12}}\,,$$
$$\sin^2\widetilde{\theta}_{12} \simeq \frac{(\alpha-\beta)\sin^2\theta_{12}}{\alpha+\beta\cos2\theta_{12}}\,. \quad (9)$$

Accordingly, we are left with

$$\cos2\widetilde{\theta}_{12} \simeq \frac{\alpha\cos2\theta_{12}+\beta}{\alpha+\beta\cos2\theta_{12}} \simeq \cos2\theta_{12} + \frac{A}{\Delta_{21}}\sin^2\theta_{12}\,, \quad (10)$$

and

$$\sin^2 2\widetilde{\theta}_{12} \simeq \frac{(\alpha^2-\beta^2)\sin^2 2\theta_{12}}{(\alpha+\beta\cos2\theta_{12})^2}$$
$$\simeq \sin^2 2\theta_{12}\left(1 - 2\frac{A}{\Delta_{21}}\cos2\theta_{12}\right)\,, \quad (11)$$

which are associated with a determination of the sign of Δ_{31} and with a precision measurement of the value of θ_{12}, respectively. Note that Eqs. (8)—(11) are valid no matter whether the neutrino mass ordering is normal or inverted. We see that the matter-induced correction is clearly characterized by the ratio

$$\frac{A}{\Delta_{21}} \simeq 1.05\times10^{-2}\times\frac{E}{4\ \text{MeV}}\times\frac{7.5\times10^{-5}\ \text{eV}^2}{\Delta_{21}}\,. \quad (12)$$

Therefore, we conclude that the precision measurements to be carried out at JUNO and RENO-50 may suffer from terrestrial matter contamination at the 1% level.

We proceed to calculate the matter-induced correction to the probability of $\overline{\nu}_{\rm e} \to \overline{\nu}_{\rm e}$ oscillations. In vacuum, we have $P(\overline{\nu}_{\rm e} \to \overline{\nu}_{\rm e}) = 1 - P_0 - P_*$ with [19]

$$P_0 = \sin^2 2\theta_{12}\cos^4\theta_{13}\sin^2 F_{21}$$
$$P_* = \frac{1}{2}\sin^2 2\theta_{13}\left(1 - \cos F_*\cos F_{21} + \cos2\theta_{12}\sin F_*\sin F_{21}\right)\,, \quad (13)$$

where $F_{ji} \equiv 1267\times\Delta_{ji}L/E$ with Δ_{ji} being the neutrino mass-squared difference in unit of eV^2, L being the baseline length in unit of km and E being the antineutrino beam energy in unit of MeV (for $ji = 21, 31, 32$), and

$$F_* \equiv F_{31} + F_{32} = 1267\times\frac{L}{E}\left(\Delta_{31}+\Delta_{32}\right) = 1267\times\frac{L}{E}\Delta_* \quad (14)$$

with the definition $\Delta_* \equiv \Delta_{31} + \Delta_{32}$. Needless to say, Δ_* must be positive (or negative) if the neutrino mass ordering is normal (or inverted). Exactly parallel with Eq. (13), the expression of $\widetilde{P}(\overline{\nu}_{\rm e} \to \overline{\nu}_{\rm e})$ in matter can be written as $\widetilde{P}(\overline{\nu}_{\rm e} \to \overline{\nu}_{\rm e}) = 1 - \widetilde{P}_0 - \widetilde{P}_*$ with

$$\widetilde{P}_0 = \sin^2 2\widetilde{\theta}_{12}\cos^4\widetilde{\theta}_{13}\sin^2\widetilde{F}_{21}$$
$$\widetilde{P}_* = \frac{1}{2}\sin^2 2\widetilde{\theta}_{13}\left(1 - \cos\widetilde{F}_*\cos\widetilde{F}_{21} + \cos2\widetilde{\theta}_{12}\sin\widetilde{F}_*\sin\widetilde{F}_{21}\right)\,, \quad (15)$$

where $\widetilde{F}_{ji} \equiv 1267\times\widetilde{\Delta}_{ji}L/E$ with $\widetilde{\Delta}_{ji}$ being the effective neutrino mass-squared difference (for $ji = 21, 31, 32$), and

$$\widetilde{F}_* \equiv \widetilde{F}_{31} + \widetilde{F}_{32} = 1267\times\frac{L}{E}\left(\widetilde{\Delta}_{31}+\widetilde{\Delta}_{32}\right) = 1267\times\frac{L}{E}\widetilde{\Delta}_* \quad (16)$$

with the definition $\widetilde{\Delta}_* \equiv \widetilde{\Delta}_{31} + \widetilde{\Delta}_{32}$. With the help of Eq. (3), we find that $\widetilde{\Delta}_{21}$ and $\widetilde{\Delta}_*$ can approximate to

$$\widetilde{\Delta}_{21} \simeq \Delta_{21} + A\cos2\theta_{12}\,, \qquad \widetilde{\Delta}_* \simeq \Delta_* + A\,, \quad (17)$$

[2] For the JUNO (or RENO-50) experiment, whose baseline length is much shorter than accelerator-based long-baseline neutrino oscillation experiments, it might be more appropriate to take a somewhat smaller value of ρ. This issue will be addressed later.

respectively. Then Eq. (15) can be explicitly expressed as

$$\begin{aligned}\widetilde{P}_0 &\simeq P_0 + A\sin^2 2\theta_{12}\cos 2\theta_{12}\cos^4\theta_{13} \\ &\quad\cdot\left(1267\frac{L}{E}\sin 2F_{21} - \frac{2}{\Delta_{21}}\sin^2 F_{21}\right) \\ \widetilde{P}_* &\simeq P_* + \frac{1}{2}A\sin^2 2\theta_{13}\left\{1267\frac{L}{E}[(1+\cos^2 2\theta_{12}) \right. \\ &\quad\cdot\sin F_*\cos F_{21} + 2\cos 2\theta_{12}\cos F_*\sin F_{21}] \\ &\quad\left. + \frac{1}{\Delta_{21}}\sin^2\theta_{12}\sin F_*\sin F_{21}\right\}, \end{aligned} \tag{18}$$

where $F_{21} = 1267\Delta_{21}L/E \sim \pi/2$ (or equivalently, $L \sim 50$ km) has been implied in accordance with the designs of the JUNO [1, 2] and RENO-50 [5] experiments, and hence $1267AL/E \sim A/\Delta_{21} \sim 10^{-2}$ is a small expansion parameter. The difference

$$\widetilde{P}(\overline{\nu}_e \to \overline{\nu}_e) - P(\overline{\nu}_e \to \overline{\nu}_e) = \left(P_0 - \widetilde{P}_0\right) + \left(P_* - \widetilde{P}_*\right), \tag{19}$$

which is proportional to A as shown in Eq. (18), is therefore a clear measure of the terrestrial matter effects associated with JUNO or RENO-50.

3 Numerical simulation

Now we turn to a numerical study of the terrestrial matter effects in a medium-baseline reactor antineutrino oscillation experiment like JUNO or RENO-50. For simplicity and illustration, we adopt the best-fit values $\Delta_{21} \simeq 7.5\times10^{-5}$ eV^2, $\Delta_* \simeq 4.839\times10^{-3}$ eV^2, $\sin^2\theta_{12} \simeq 0.304$ and $\sin^2\theta_{13} \simeq 0.0218$ obtained from a recent global analysis of current neutrino oscillation data [18]. The terrestrial matter density along the antineutrino trajectory is typically assumed to be $\rho \simeq 2.6$ g/cm^3, and its uncertainty will be briefly discussed later on. In our analysis we are going to focus on the normal neutrino mass ordering as the true mass ordering, and we find that our main conclusion will actually remain valid even if the inverted neutrino mass ordering is taken into account.

As a result of our exact numerical calculations without involving any analytical approximations, Fig. 1 shows the absolute (a) and relative (b) differences between the matter-corrected probability $\widetilde{P}(\overline{\nu}_e \to \overline{\nu}_e)$ and its vacuum counterpart $P(\overline{\nu}_e \to \overline{\nu}_e)$ associated with a medium-baseline ($L = 52.5$ km) reactor antineutrino oscillation experiment. The solid curves are for the true antineutrino energy, and the dashed ones are averaged over a Gaussian energy resolution of $3\%/\sqrt{E\,(\mathrm{MeV})}$. We see that the absolute difference $\widetilde{P}(\overline{\nu}_e \to \overline{\nu}_e) - P(\overline{\nu}_e \to \overline{\nu}_e)$ can reach about 0.7% in the vicinity of the first oscillation peak of Δ_{21}, which corresponds to a relative matter-induced correction of about 4% as illustrated in Fig. 1(b). As a matter of fact, the main profile of $\widetilde{P}(\overline{\nu}_e \to \overline{\nu}_e) - P(\overline{\nu}_e \to \overline{\nu}_e)$ or $\left[\widetilde{P}(\overline{\nu}_e \to \overline{\nu}_e) - P(\overline{\nu}_e \to \overline{\nu}_e)\right]/\widetilde{P}(\overline{\nu}_e \to \overline{\nu}_e)$ is attributed to the Δ_{21}-triggered oscillation, where the matter-induced suppression in $\sin^2 2\widetilde{\theta}_{12}$ provides a positive correction in the Δ_{21}-dominated range. The small wiggles in Fig. 1 are caused by the Δ_*-triggered oscillation, and their amplitudes are modulated by the energy-dependent correction of $\cos 2\widetilde{\theta}_{12}$.

Before calculating the statistical sensitivity of a realistic experimental measurement, it is necessary to test the accuracy of our analytical approximations made in Eqs. (8)–(11) and Eqs. (15)–(18). Figure 2 shows a comparison between the results of $\widetilde{P}(\overline{\nu}_e \to \overline{\nu}_e)$ obtained from a complete numerical calculation and the analytical approximations made in Eq. (18): their absolute (a) and relative (b) differences with or without smearing effects for a reactor antineutrino oscillation experiment like JUNO or RENO-50. In this figure the solid lines are for the true antineutrino energy, and the dashed curves are averaged over a Gaussian energy resolution of $3\%/\sqrt{E\,(\mathrm{MeV})}$. We find that the absolute errors of our analytical approximations are lower than 3×10^{-4} in

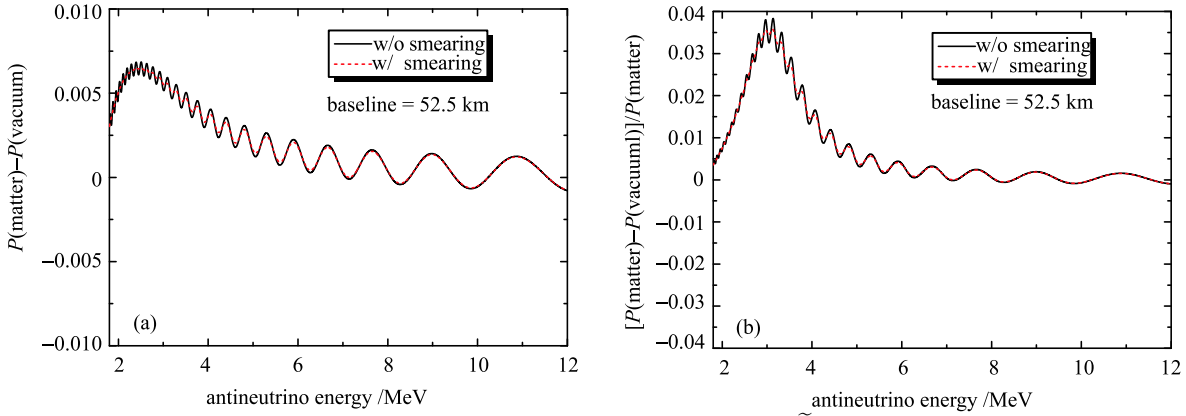

Fig. 1. (color online) The absolute (a) and relative (b) differences between $\widetilde{P}(\overline{\nu}_e \to \overline{\nu}_e)$ (in matter) and $P(\overline{\nu}_e \to \overline{\nu}_e)$ (in vacuum) for a reactor antineutrino oscillation experiment with $L = 52.5$ km. The solid lines correspond to the true antineutrino energy, and the dashed lines are averaged over a Gaussian energy resolution of $3\%/\sqrt{E\,(\mathrm{MeV})}$.

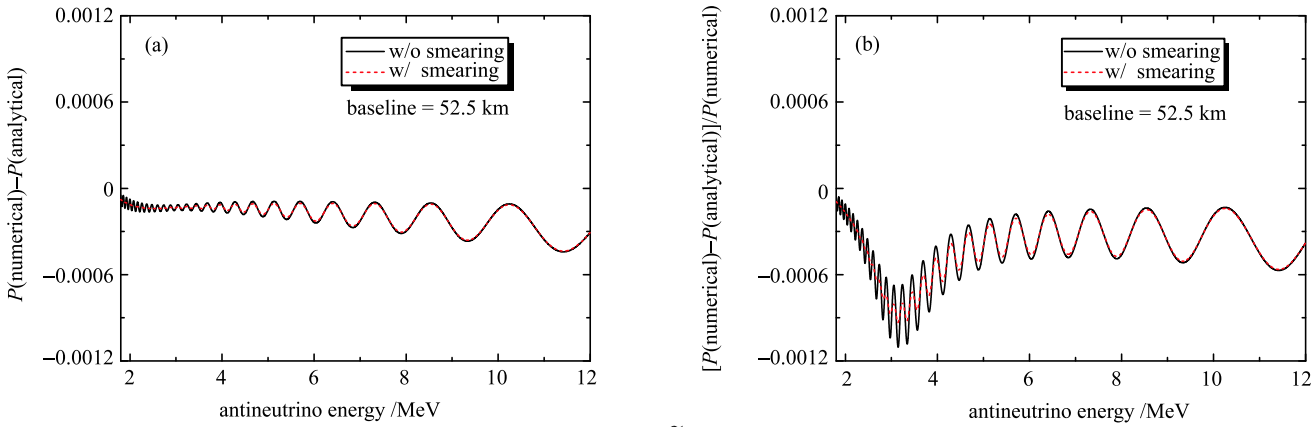

Fig. 2. (color online) Comparison between the results of $\widetilde{P}(\overline{\nu}_e \to \overline{\nu}_e)$ achieved from an exact numerical calculation (numerical) and from the analytical approximations in Eq. (18) (analytical): their absolute (a) and relative (b) differences with or without smearing for a reactor antineutrino oscillation experiment with $L = 52.5$ km. The solid curves are for the true antineutrino energy, and the dashed ones are averaged over a Gaussian energy resolution of $3\%/\sqrt{E\,(\mathrm{MeV})}$.

most of the antineutrino energy range, proving that Eq. (18) and the associated analytical approximations can be safely employed in the following sensitivity studies.

Taking account of JUNO's nominal setup as described in Refs. [1, 20], we are going to illustrate how the terrestrial matter effects influence the measurements of both the neutrino mass ordering and the flavor mixing parameters. We shall also discuss an important issue: to what extent one can establish or constrain the terrestrial matter effects at JUNO or RENO-50, or in a similar experiment to be proposed.

Given the JUNO simulation, which has been described in detail in Ref. [1], let us consider a 20 kt liquid scintillator detector with an energy resolution of $3\%/\sqrt{E\,(\mathrm{MeV})}$ [1)]. We take account of the real reactor powers and baseline distributions of the Yangjiang and Taishan nuclear power plants listed in Table 2 of Ref. [1], which have a total thermal power of 36 $\mathrm{GW_{th}}$ and a power-weighted baseline of 52.5 km. Moreover, we assume a detection efficiency of 80% and a nominal running time of six years and 300 effective days per year in our numerical simulation.

To discuss the statistical sensitivity of the experimental measurement [2)], we construct the following standard χ^2 function:

$$\chi^2 = \sum_{i=1}^{N_{\rm bin}} \frac{\left[M_i(p^M,\eta) - T_i(p^T,\eta)\left(1+\sum_k \alpha_{ik}\epsilon_k\right)\right]^2}{M_i(p^M,\eta)} + \sum_k \frac{\epsilon_k^2}{\sigma_k^2}\,, \tag{20}$$

where M_i and T_i are the measured and predicted antineutrino events in the i-th antineutrino energy bin, respectively; σ_k and ϵ_k are the k-th systematic uncertainty and the corresponding pull parameter, respectively. The considered nominal systematic uncertainties include the correlated reactor rate uncertainty ($\sim 2\%$), the uncorrelated reactor rate uncertainty ($\sim 0.8\%$), the energy-uncorrelated bin-to-bin reactor flux spectrum uncertainty ($\sim 1\%$) and the detector-related uncertainty ($\sim 1\%$). Some additional important systematic uncertainties on the measurements of the neutrino mass ordering and oscillation parameters have been thoroughly discussed in sections 2 and 3 of Ref. [1]. In Eq. (20), p stands for the oscillation parameters (i.e., $p = \{\Delta_{21}, \Delta_*, \theta_{12}, \theta_{13}\}$), and $\eta \equiv A(\rho)/A(\rho = 2.6\,\mathrm{g/cm^3})$ is defined as the effective matter potential index.

Figure 3 is a comparison of the neutrino mass ordering sensitivities with (solid) and without (dashed) considering the terrestrial matter effects. The black lines come from the fitting in the assumption of the normal

[1)] A generic parametrization of the energy resolution is written as $\sqrt{(a/\sqrt{E})^2 + b^2 + (c/E)^2}$, which is numerically equivalent to an effective energy resolution of $\sqrt{a^2 + (1.6\times b)^2 + (c/1.6)^2}/\sqrt{E}$ in the mass ordering measurement [1]. The requirement of $3\%/\sqrt{E\,(\mathrm{MeV})}$ can be regarded as the total contribution of all the stochastic and non-stochastic terms.

[2)] See Refs. [1, 20–25] for an incomplete list of the works dealing with the statistical sensitivity of the mass ordering measurement in a medium-baseline reactor antineutrino experiment.

mass ordering (NMO) of three neutrinos, and the red lines assume the inverted mass ordering (IMO). The vertical distance between the minima of the red and black curves is defined as a measure of the neutrino mass ordering sensitivity:

$$\Delta\chi^2_{\rm MO} = |\chi^2_{\rm min}({\rm NMO}) - \chi^2_{\rm min}({\rm IMO})| \ , \qquad (21)$$

where the minimization is implemented for all the relevant oscillation and pull parameters. Compared with the situation of $\overline{\nu}_{\rm e} \to \overline{\nu}_{\rm e}$ oscillations in vacuum, the inclusion of terrestrial matter effects may reduce the value of $\Delta\chi^2_{\rm MO}$ from 10.28 to 9.64, which is comparable with other important systematic uncertainties and hence should not be neglected in the future mass ordering measurement. In the above calculation we have typically taken $\rho \simeq 2.6\,{\rm g/cm^3}$ for the terrestrial matter density. For reactor antineutrino oscillations with a medium baseline (i.e., $L \sim 50$ km from the reactors to the detector), however, the $\overline{\nu}_{\rm e}$ trajectory during propagation is expected to include a large proportion of the sedimentary layer. In other words, the real experiment may actually involve a somewhat smaller terrestrial matter density. In Fig. 4 we illustrate the sensitivity of the mass ordering measurement $\Delta\chi^2_{\rm MO}$ as a function of the matter potential index η. One can see that $\Delta\chi^2_{\rm MO}$ depends linearly on η. If a smaller matter density $\rho \simeq 2.0\,{\rm g/cm^3}$ is taken into account for JUNO, the mass ordering sensitivity will be reduced from 10.28 to 9.79.

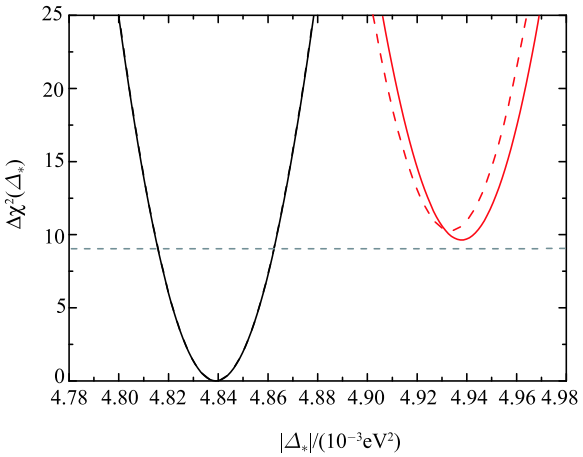

Fig. 3. (color online) Comparison of the neutrino mass ordering sensitivities with (red solid) and without (red dashed) considering the terrestrial matter effects. The vertical distance (defined as $\Delta\chi^2_{\rm MO}$) between the minima of the red and black lines denotes the sensitivity of the mass ordering measurement.

Now we turn to discuss the terrestrial matter effects on the relevant flavor parameters. In our numerical analysis, $\rho \simeq 2.6\,{\rm g/cm^3}$ (i.e., $\eta \simeq 1$) is typically taken to modulate the measured antineutrino events M_i. In Fig. 5(a) we include terrestrial matter effects in the predicted antineutrino events T_i and display the fitting results of Δ_{21} and θ_{12}. The red star denotes the true values of these two parameters. It turns out that the best-fit points can return to the true values, and the allowed regions are consistent with the fitting results in the assumption of the vacuum $\overline{\nu}_{\rm e} \to \overline{\nu}_{\rm e}$ oscillations (see section 3.2 of Ref. [1]). The 1σ precision levels of Δ_{21} and $\sin^2\theta_{12}$ with the nominal systematic setup can reach 0.23% and 0.58%, respectively. In comparison, the 1σ precision levels of Δ_{21} and $\sin^2\theta_{12}$ in the absence of matter effects were found to be 0.24% and 0.54%, respectively (see section 3.2 of Ref. [1]). A minor reduction in the accuracy of $\sin^2\theta_{12}$ is certainly attributed to the suppression of θ_{12} in terrestrial matter.

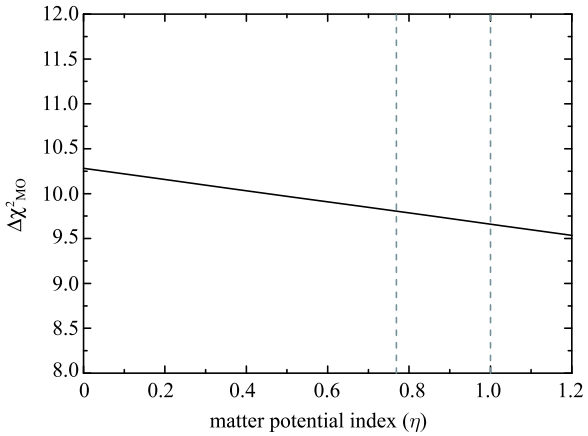

Fig. 4. Sensitivity of the mass ordering measurement $\Delta\chi^2_{\rm MO}$ as a function of the matter potential index $\eta \equiv A(\rho)/A(\rho = 2.6\ {\rm g/cm^3})$. The vertical dashed line with $\eta \simeq 1$ or 0.77 stands for the terrestrial matter density $\rho \simeq 2.6\,{\rm g/cm^3}$ or $2.0\,{\rm g/cm^3}$, respectively. The value of $\Delta\chi^2_{\rm MO}$ for $\eta \simeq 0$, 0.77 or 1 is 10.28, 9.79 or 9.64, respectively.

For the sake of comparison, let us neglect terrestrial matter effects in the predicted antineutrino events T_i and illustrate the fitting results of Δ_{21} and θ_{12} in Fig. 5(b). The red star points to the true values of these two parameters, and the blue dot stands for the best-fit point. The allowed regions are shifted to higher Δ_{21} and lower θ_{12}, and the best-fit point is located at $\Delta_{21} \simeq 7.514\times10^{-5}\,{\rm eV}^2$ and $\theta_{12} \simeq 33.26^\circ$. The precision of Δ_{21} and θ_{12} turns out to be the same as that in Fig. 5(a). Hence the best-fit values of Δ_{21} and θ_{12} deviate around 0.8σ and 2.4σ from their true values, respectively. If additional systematic uncertainties [1] of the flux spectrum and the energy scale are taken into account in the analysis, the sizes of the deviations might be reduced.

Finally let us discuss to what extent one can establish or constrain the terrestrial matter effects at JUNO. Assuming a matter density $\rho \simeq 2.6\,{\rm g/cm^3}$ in the measured antineutrino events, we illustrate the change of $\Delta\chi^2(\eta)$

as a function of the matter potential index η in Fig. 6 with both fixed and free oscillation parameters. If all the oscillation parameters are fixed, we obtain $\Delta\chi^2(0) \simeq 11$, indicating that the terrestrial matter effects can be tested with a significance of more than 3σ. However, the significance of establishing the terrestrial matter effects will significantly reduce to 1.3σ after the oscillation parameters are marginalized. This can be understood with the help of Eqs. (11) and (17), where the corrections of the matter potential to $\sin^2\theta_{12}$ and Δ_{21} are about 0.8% and 0.4%, respectively. If some additional systematic uncertainties are considered in the analysis [1], including the background, the reactor flux spectrum uncertainty of 1%, the energy scale uncertainty of 1% and the energy non-linear uncertainty of 1%, then the projected precision levels for $\sin^2\theta_{12}$ and Δ_{21} will be 0.72% and 0.60%, respectively. Correspondingly, the sensitivity of establishing the terrestrial matter effects will be less than 1σ.

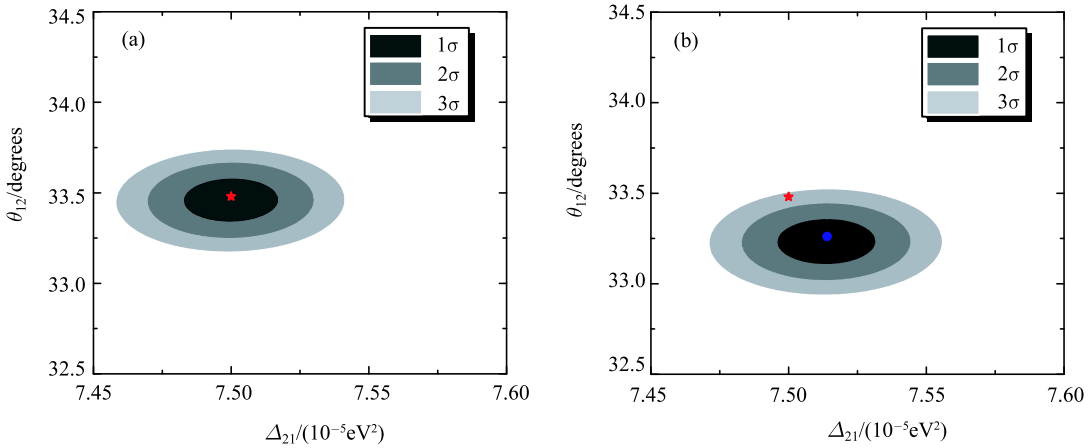

Fig. 5. (color online) The allowed regions of Δ_{21} and θ_{12} with (a) and without (b) including terrestrial matter effects in the predictions. The matter density $\rho \simeq 2.6\,\mathrm{g/cm^3}$ is assumed in the measurements. The red stars denote the true values of Δ_{21} and θ_{12}, and the blue dot is the best-fit point when the terrestrial matter effects are omitted.

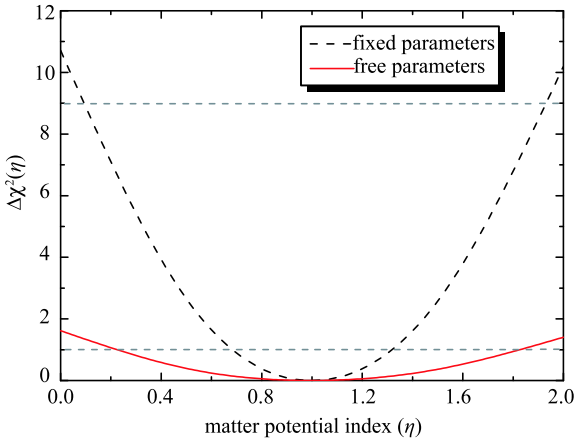

Fig. 6. (color online) Sensitivity of the terrestrial matter effects with the JUNO nominal setup. The black dashed and red solid lines are shown for the fitting results without and with considering the uncertainties of the neutrino oscillation parameters, respectively.

If near detectors can be built to monitor the reactor antineutrino flux, a relative measurement of the rate and spectrum between the near and far detectors is expected to significantly reduce the reactor- and detector-related systematic uncertainties in the $\sin^2\theta_{12}$ and Δ_{21} measurements, and thus the sensitivity of establishing the terrestrial matter effects can accordingly increase. Without specifying the details of the near detectors, we just split the systematic uncertainties into the (detector-correlated) absolute uncertainties and (detector-uncorrelated) relative uncertainties. Assuming the absolute errors will be cancelled by virtue of the near detectors and the relative errors are at the Daya Bay level [26–29], we show the sensitivity of ruling out the vacuum neutrino oscillation scenario (i.e., $\eta = 0$) as a function of the running time in Fig. 7, where the significance is defined as the square root of $\Delta\chi^2(\eta = 0)$. We observe that a 2σ sensitivity of establishing the terrestrial matter effects can be achieved for about 10 years of data taking, if one or two appropriate near detectors are implemented to the nominal JUNO configuration. Further details on the near detector configuration will be discussed elsewhere[1)].

4 Concluding remarks

To summarize, we have examined how small the terrestrial matter effects can be in a medium-baseline

[1)] Given different motivation and different detector consideration, there are a few other works on the near detector ideas for a medium-baseline reactor antineutrino oscillation experiment [30–32].

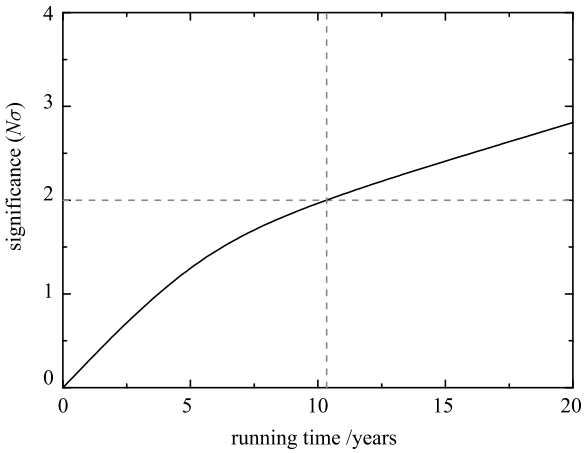

Fig. 7. Sensitivity of ruling out the vacuum neutrino oscillation scenario (i.e., $\eta=0$) as a function of running time with the nominal JUNO configuration and appropriate near detectors. The significance is defined as the square root of $\Delta\chi^2(\eta=0)$.

reactor antineutrino oscillation experiment like JUNO or RENO-50, which aims to carry out a precision measurement of the neutrino mass ordering and relevant flavor parameters. To do so, we have expanded the probability of $\overline{\nu}_{\rm e}\to\overline{\nu}_{\rm e}$ oscillations with $L\simeq 50$ km in terms of the small matter parameter. Our analytical approximations are simple but accurate enough for a deeper understanding of the outputs of the exact numerical calculations. Taking the JUNO experiment, which is currently under development, as a good example, we have shown that the inclusion of terrestrial matter effects is likely to reduce the sensitivity of the neutrino mass ordering measurement by $\Delta\chi^2_{\rm MO}\simeq 0.6$. We find that the terrestrial matter effects may also shift the best-fit values of θ_{12} and Δ_{21} by about 1σ to 2σ if they are ignored in future data analyses.

We conclude that the terrestrial matter effects must be carefully taken into account because they are non-negligible in the reactor-based measurements of the neutrino mass ordering and $\overline{\nu}_{\rm e}\to\overline{\nu}_{\rm e}$ oscillation parameters. But it remains difficult to establish the profile of terrestrial matter effects at a high significance level in a realistic experiment of this kind, such as JUNO or RENO-50. This issue motivates us to consider the possibility of installing near detectors to measure the initial reactor antineutrino flux [1)], in a location where the matter effects are not present. In this case a comparison between the measurement of $\widetilde{P}(\overline{\nu}_{\rm e}\to\overline{\nu}_{\rm e})$ and its energy dependence at the far detector ($L\simeq 50$ km) and that of $P(\overline{\nu}_{\rm e}\to\overline{\nu}_{\rm e})$ at the near detectors ($L\sim 0$) will allow one to probe the fine effects of terrestrial matter associated with JUNO or RENO-50. Our preliminary estimate indicates that it is possible to establish the terrestrial matter effects with a 2σ sensitivity for about 10 years of data taking at JUNO with the help of a suitable near detector implementation.

We thank Eligio Lisi, Shun Zhou and Jing-yu Zhu for useful discussions.

References

1 F. An et al (JUNO Collaboration), J. Phys. G, **43**: 030401 (2006)
2 Z. Djurcic et al (JUNO Collaboration), arXiv:1508.07166
3 X. Qian and P. Vogel, Prog. Part. Nucl. Phys., **83**: 1 (2015)
4 R. B. Patterson, Ann. Rev. Nucl. Part. Sci., **65**: 177 (2015)
5 S. B. Kim, Nucl. Part. Phys. Proc., **265**–**266**: 93 (2015)
6 F. Capozzi, E. Lisi and A. Marrone, Phys. Rev. D, **89**: 013001 (2014)
7 Y. F. Li and Y. L. Zhou, Nucl. Phys. B, **888**: 137 (2014); Y. F. Li, in section 3.2 of Ref. [1].
8 F. Capozzi, E. Lisi, and A. Marrone, Phys. Rev. D, **92**: 093011 (2015)
9 L. Wolfenstein, Phys. Rev. D, **17**: 2369 (1978)
10 S. P. Mikheev and A. Y. Smirnov, Sov. J. Nucl. Phys., **42**: 913 (1985) [Yad. Fiz., **42**: 1441 (1985)]
11 H. Zhang and Z. Z. Xing, Eur. Phys. J. C, **41**: 143 (2005)
12 Z. Z. Xing and J. Y. Zhu, JHEP, **1607**: 011 (2016)
13 I. Mocioiu and R. Shrock, Phys. Rev. D, **62**: 053017 (2000)
14 K. A. Olive et al (Particle Data Group Collaboration), Chin. Phys. C, **38**: 090001 (2014)
15 F. Capozzi, G. L. Fogli, E. Lisi et al, Phys. Rev. D, **89**: 093018 (2014)
16 F. Capozzi, E. Lisi, A. Marrone et al, Nucl. Phys. B, **908**: 218 (2016)
17 D. V. Forero, M. Tortola, and J. W. F. Valle, Phys. Rev. D, **90**: 093006 (2014)
18 M. C. Gonzalez-Garcia, M. Maltoni, and T. Schwetz, JHEP, **1411**: 052 (2014)
19 Y. Wang and Z. Z. Xing, arXiv:1504.06155
20 Y. F. Li, J. Cao, Y. Wang, and L. Zhan, Phys. Rev. D, **88**: 013008 (2013)
21 X. Qian, D. A. Dwyer, R. D. McKeown et al, Phys. Rev. D, **87**: 033005 (2013)
22 S. F. Ge, K. Hagiwara, N. Okamura, and Y. Takaesu, JHEP, **1305**: 131 (2013)
23 E. Ciuffoli, J. Evslin, and X. Zhang, Phys. Rev. D, **88**: 033017 (2013)
24 M. Blennow, P. Coloma, P. Huber, and T. Schwetz, JHEP, **1403**: 028 (2014)
25 M. Y. Pac, Nucl. Phys. B, **902**: 326 (2016)
26 F. P. An et al (Daya Bay Collaboration), Phys. Rev. Lett., **108**: 171803 (2012)
27 F. P. An et al (Daya Bay Collaboration), Chin. Phys. C, **37**: 011001 (2013)
28 F. P. An et al (Daya Bay Collaboration), Phys. Rev. Lett., **112**: 061801 (2014)
29 F. P. An et al (Daya Bay Collaboration), Phys. Rev. Lett., **115**: 111802 (2015)
30 A. B. Balantekin et al, arXiv:1307.7419
31 E. Ciuffoli, J. Evslin, Z. Wang et al, Phys. Rev. D, **89**: 073006 (2014)
32 H. Wang, L. Zhan, Y. F. Li et al, arXiv: 1602.04442

[1)] We thank Jun Cao for useful communication in this connection.